Monte Carlo simulation of controlled impurity diffusion in semiconductors using split gates

V. Narayan and M. Willander
Physical Electronics and Photonics, Department of Physics, Fysikgränd 3, University of Göteborg and Chalmers University of Technology, S-412 96 Göteborg, Sweden

(Received 13 June 2001; revised manuscript received 28 September 2001; published 22 January 2002)

We propose an experiment, where impurity diffusion in a semiconductor layer during heat treatment, can be controlled by a nonlinear potential produced by split gates. We approximated the nonlinear potential as a parabola centered at the middle of the semiconductor layer; the impurities diffuse into the central region. Starting with the phenomenological Arrhenius equation, we describe a simple model for the impurity diffusion, and then perform Monte Carlo simulations to predict the impurity profile, for different parabolic constants and impurity densities. The results show that charge builds up in the central area creating a long-range internal electric field. The internal field at high doping levels, can be of sufficient strength to cause the broadening of the impurity density profile. The width of the impurity profile can be controlled by the curvature of the parabola, which in turn depends on the split-gate geometry and voltage.

DOI: 10.1103/PhysRevB.65.075308 PACS number(s): 66.30.Jt, 61.72.Tt

I. INTRODUCTION

The fundamental physics of impurity diffusion in semiconductors has great significance for technology, since it is a critical step in the fabrication of many devices. The impurities (either acceptors or donors) ionize at high temperatures, then diffuse through the crystal. The empirical evidence[1] shows impurity diffusion is well described by an Arrhenius equation. There are many theories[2–4] more physical than earlier simpler models,[5–8] that explain the Arrhenius behavior. Recently, density-functional theory has been used to estimate diffusion activation energies, and reasonable agreement with experiment has been obtained.[9] Given the impurities are charged particles, an applied electric field will favor hopping to the direction of lower potential.[10,11] The use of electric fields to influence doping profiles goes back to the early days of semiconductor science with the control of impurity diffusion in silicon and germanium.[12–14] Recently, forced diffusion by strong electric fields[15,16] has been employed in diamond to *n* dope this material. It has been pointed out that forced diffusion has the advantage over ion implantation as it avoids damaging the crystal structure and allows diffusion to take place at lower temperatures.[17,18]

In this paper we propose and model an experiment where impurity density profiles are localized in a region of space in one dimension. The impurity diffusion is controlled using a nonlinear potential produced by split-gates. A split-gate configuration[19] can produce an external potential with an approximate harmonic form in one dimension. Several split gates can be orientated to achieve impurity diffusion control in further direction(s). In principle, one is not restricted to using split gates, a square gate[20] may be used that produces a harmonic potential in two directions, or perhaps more intricate configurations can be employed.

The central equation of our model is an Arrhenius equation describing the diffusion process. The Arrhenius equation is modified to include the position-dependent potential, to derive the position-dependent hopping probabilities. The impurities without the field have equal chance to hop in all directions. The potential biases the hopping towards lower potential, the minimum energy point being the minima of the external parabolic potential. We perform a 1D (one dimensional) Monte Carlo simulation to determine the doping density profile. The nonhomogeneous distribution of impurities give rise to an internal potential that resists the build up of charge in the locality of the minima of the external parabolic potential. The internal potential is calculated using the Poisson equation and the discrete nature of the impurities are neglected. A more accurate discrete description of the internal potential suggests that large random potentials can occur near the vicinity of a given impurity during diffusion,[21] we discuss this point later in the paper. The ideas described could be applied during device fabrication in the future, but it is first necessary to successfully demonstrate the reality of controlled impurity diffusion.

II. A PROPOSED PILOT EXPERIMENT TO DEMONSTRATE CONTROLLED IMPURITY DIFFUSION

The structure for the experiment is infinitely long in the *z* direction whose cross section is schematically shown in Fig. 1. In the *y* direction we have a series of semiconductor/oxide layers that produces a double barrier structure in the conduction band. These layers have finite width of the order 30 nm in the *x* direction. The oxide barriers define a central semiconductor quantum wire (which is initially evenly *n* doped) of width $2L$ in the *y* direction. There are metal split gates grown on top, separated by an oxide layer to prevent charge flow into the semiconductor. The structure must rest on a substrate with a groove allowing the doped region in the *x* direction to be exposed to the vacuum. Alternatively, the structure may be reorientated 180° and placed on a flat oxide substrate. The gates are kept at fixed equal voltage V_g and an approximate parabolic potential is produced centered at the middle of the semiconductor layer. The structure is heated and the donors ionize. The external voltage V_{ext} in the *y* direction in the central semiconductor layer formed from the split gates, shall be approximated as harmonic with the form

$$V_{ext}(y) = ay^2, \tag{1}$$

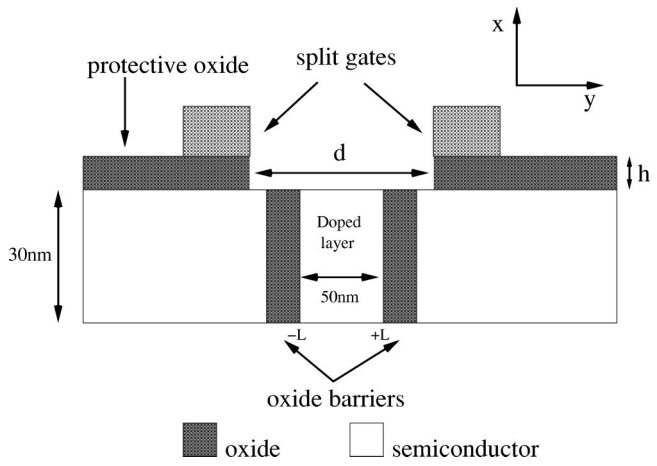

FIG. 1. The schematic diagram of the proposed experiment. We show a cross section in the *x*-*y* plane of a structure that extends to infinity in the *z* direction. There are two oxide layers embedded in a crystalline semiconductor heterostructure layer with finite width in the *x* direction. The oxide layers define a central semiconductor layer in the *y* direction with width $2L$. The metal split gates are separated from the semiconductor by a protective oxide layer that prevents charge transfer to the semiconductor. The field effect produced by the gates produces a potential that has an approximate parabolic form in the *y* direction centered in the middle of the semiconductor layer. The separation *d* between the split gates, the height *h* of the protective oxide layer, and the gate voltage V_g can be varied to tailor the curvature of the parabola.

where *a* is a constant. We have assumed the potential produced by the gates in the doped layer varies very little with *x* coordinate. This can be achieved with suitable gate and device dimensions.[19] The value of the constant *a* can be altered by changes to the split-gate voltage V_g, the distance *d* between the split gates, and the height *h* of the protective oxide layers.

The impurities are chosen such that the diffusion energy barrier is low enough to let impurities diffuse with reasonable time at the processing temperature. At high enough temperatures, impurities diffusing through interstitial and other mechanisms are suitable for the experiment. The external potential initially drives net impurity migration to the center of the doped layer in the *y* direction. The electrons experience a force in the opposite direction compared to the positive impurities. The conduction-band profile in the *y* direction resembles a ''hill'' and electrons may tunnel through the oxide layers into the left and right semiconductor layers, leaving the doped region positively charged. The impurities are free to move in the *x* and *z* directions within the crystal. The sample is kept at constant temperature (perhaps for several hours) until the impurity density profile has stabilized and reached equilibrium.

The oxide layers next to the doped semiconductor layer are not necessary in the experiment, but their presence could be useful for device fabrication, post heat treatment. The sample could be exposed to a standard etchant to remove the oxide regions. The split gates can then be removed and source and drain can be grown next to the doped semiconductor layer by CVD (chemical vapor deposition). The device processing should take place at relatively low temperatures and quickly as possible, leaving the controlled impurity profile relatively undisturbed. The impurity profile will largely determine the *I*-*V* (current-voltage) characteristics of a particular device. The details and characteristics of possible future devices or improved existing devices are beyond the scope of this paper; we aim to theoretically demonstrate the feasibility of controlled impurity diffusion.

III. THE IMPURITY DIFFUSION WITH A POSITION-DEPENDANT POTENTIAL

We first discuss the simplest case, impurities diffusing in the absence of an external potential for when the impurity-impurity Coulomb interaction is ignored. The model is later modified to include the external potential as well as an approximation to the impurity-impurity interaction. We assume the impurities are reflected at the interfaces with the oxide. The oxide could be doped with a diffusion inhibiting element such as nitrogen that retards boron diffusion in silicon, and/or the oxide could be polycrystalline. The diffusion through the oxide is assumed to be much slower than diffusion through the semiconductor crystal. In any case, it is not necessary to assume reflection at the interfaces, but we choose to ignore the details of diffusion through the oxide. We consider diffusion of impurities through interstitial sites. However, this is not a necessary requirement of the experiment. The impurities hop from interstitial site to interstitial site. The probability of hopping *W* during the time interval dt has the form

$$W = D_0 \exp\left(\frac{-E_a}{k_B T}\right) dt \tag{2}$$

for $k_B T \ll E_a$, where E_a the activation energy (that represents a potential barrier to impurity diffusion) and D_0 is the diffusion constant. The hopping probability is equal in all directions, except at the interface where the particles are perfectly reflected in the *y* direction. In essence the diffusion problem is one dimensional, and can be described by a 1D Monte Carlo simulation of a number of particles hopping in a finite-sized lattice with reflecting end points. The sites of the 1D lattice defines for our problem the *y* coordinates of the impurities. The 1D Monte Carlo simulation has been solved[23,24] and the particle probability density was found to have a Gaussian distribution that showed agreement with an analytic solution of a continuum description of the diffusion.[22]

The electric field will modify Eq. (2) so that the hopping probability W_{ij} between neighboring sites *i* and *j*,

$$W_{ij} = D_0 \exp\left(\frac{-E_a - V_{ij}/2}{k_B T}\right) dt, \tag{3}$$

where V_{ij} is the total potential difference between lattice sites *i* and *j*. The potential differences V_{ij} is the sum of the external field V_{ext} produced by the split gates and the internal field V_{int} manifesting from a non homogeneous distribution of impurities. We introduce an effective temperature-dependent time $d\tau = D_0 \exp(-E_a/k_B T) dt$ and we rewrite Eq. (3) in the form

$$W_{ij} = D_0 \exp\left(\frac{V_{ij}}{2k_B T}\right) d\tau, \tag{4}$$

where the hopping probability given that the field is nonlinear is a function of position in the y direction. This added complexity prevents an analytic solution of the diffusion problem and we must use Monte Carlo simulations to determine the doping profile. The internal potential produced by the doping profile shall be calculated by ignoring the discrete nature of the impurities, we numerically solve the Poisson equation,

$$\nabla^2 V_{int}(y) = -\frac{\rho(y)}{\epsilon}, \tag{5}$$

where $\rho(y)$ is the charge density and ϵ is the static dielectric constant of the material. We impose the boundary conditions that $V_{int}=0$ and $\rho(y)=0$ for $y \to \pm\infty$. We ignore the boundary effects in the x direction, the charge density is assumed to vary only with the y direction.

The model described only takes into account the bare impurity charges, neglecting electron/hole screening effects. The electronic charge has been smeared out throughout the strcuture, to ensure charge neutrality of the system, thus allowing a physical treatment of the Poisson equation. The Debye length at typical growth temperatures and carriers densities is much larger than the intersite distance.[25] The electric field resulting from inhomogeneities in the electron/hole density will be neglible for distances much smaller than the Debye length, and can be neglected as in a previous study of impurity diffusion.[21]

The exact steps in the Monte Carlo simulation are as follows. The first step involves placing a constant distribution of impurities at each site, we choose to place 500 impurities per site. The second step involves calculating the internal potential to evaluate the total potential, to determine the left and right hopping probabilities for each site. The third step involves generating a set of random numbers and then moving the impurities. We repeat the second and third steps until the impurity density profile has converged (remains effectively static with time). The simulation takes roughly 90 seconds on a Sun Ultra 5 machine.

The Monte Carlo simulation allows considerable flexibility in modeling experiments. During device processing there are usually many steps each at a particular temperature.[26] These changes in temperature can be easily incorporated in the Monte Carlo simulation. Furthermore, processing may not last long enough for the impurity profile to reach equilibrium, and the Monte Carlo simulation can predict with reasonable accuracy these nonequilibrium doping profiles. In addition, further impurities can be introduced during the simulation at a specified rate that can be time dependent, to simulate impurities entering the sample from an impurity source.

In a future publication[27] we shall consider the case where the sample moves slowly relative to the split gates, to clean areas of semiconductor of unwanted impurities. The time dependence of the external potential can be easily incorporated in the Monte Carlo simulation. In comparison, extending numerical techniques[28,29] to include a time-dependent external potential in the coupled drift diffusion and Poisson equations is not trivial.

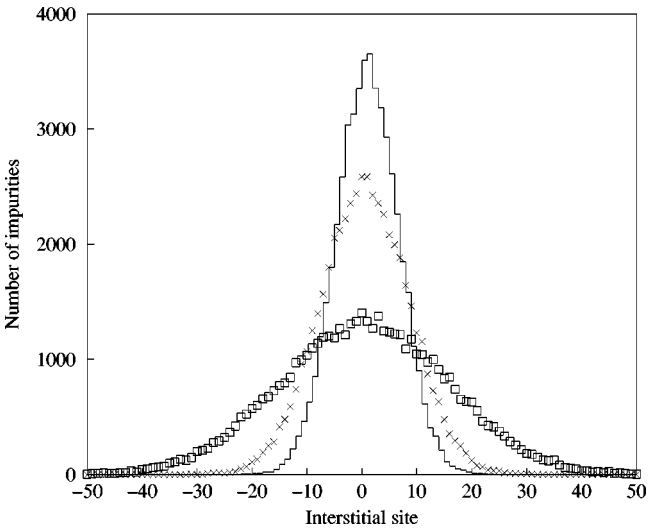

FIG. 2. The graph of the number of impurities at each interstitial site after a thousand time steps. The internal field V_{int} is not included in the simulation. The external potential at the interface $V_{ext}(L)$ produced by the split gates has the values 2.0 eV (solid lines), 1.0 eV (crosses), and 0.3 eV (boxes) respectively.

IV. NUMERICAL RESULTS

The results are presented for a 1D lattice with 101 interstitial sites with separation between sites fixed to 0.5431 nm. We set the dielectric constant $\epsilon=11.4$ the value for silicon. We set $\tau=0.37$ and $T=600$ K to allow significant probability of impurity hopping per unit time. We aim to show the general diffusion characteristics, a more detailed analysis can be performed after experiments have been performed. In Fig. 2 we show the impurity distribution after a thousand units of time for a range of values of the parabolic constant to produce $V_{ext}(L)$ between 2.0 and 0.3 eV, and we have ignored the internal field. The impurity distribution has a Gaussian profile that becomes sharper with increased curvature of the external potential. In Fig. 3 we show how the impurity diffusion profile alter when we include the effects of the internal field and set the initial impurity particle density to 10^{17} cm^{-3}, there is very little difference between the graphs, the internal field must be relatively weak.

In Fig. 4 we show how the impurity diffusion profile alters when we set the initial doping level to 10^{18} cm^{-3}. The effect of the internal field is clearly significant, the impurity density at the center has almost halved. The diffusion profile is best explained by comparing the time evolution of the impurity profile shown in Fig. 5 where the internal field is ignored, with Fig. 6 where both internal and external potentials are included. The internal field at $\tau=0$ has a constant value since the charge density is constant, and does not alter the left and right hopping probabilities. The impurity distributions are very similar at 50 time units, the doping density is still relatively constant, thus the internal potential is small.

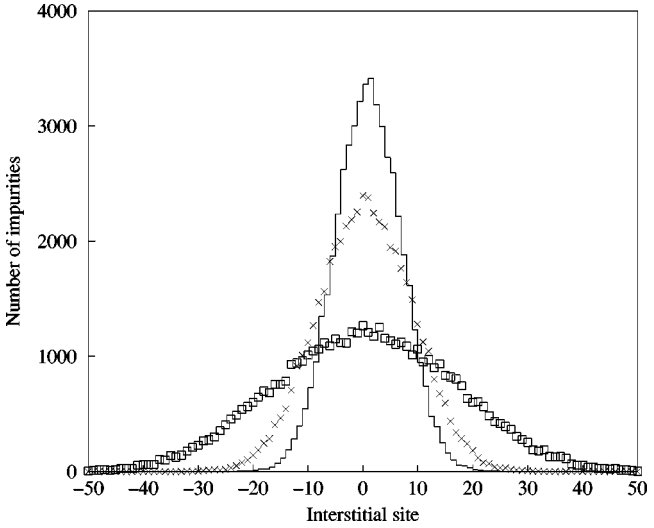

FIG. 3. The graph of the number of impurities at each interstitial site after a thousand time steps. The internal field V_{int} is included in the simulation. The doping density at the start of the simulation is set to 10^{17} cm^{-3}. The external potential at the interface $V_{ext}(L)$ produced by the split gates has the values 2.0 eV (solid lines), 1.0 eV (crosses), and 0.3 eV (boxes), respectively.

The impurities accelerated by the external field hop towards the center of the lattice and charge builds up at the central region. The impurity density profile after 100 time steps in Fig. 5 is clearly peaked at the center. As a consequence a potential is created that has a maximum at the center and falls to zero towards the edges. The internal field, therefore, causes particle to hop out of the central area, thus the impurity profile in Fig. 6 after 100 time steps is noticeably broader when compared with Fig. 5. The internal potential dominates the total potential in the central region causing

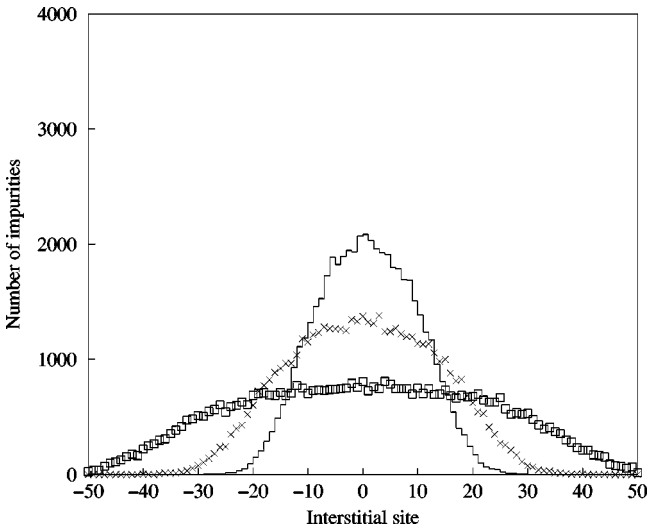

FIG. 4. The graph of the number of impurities at each interstitial site after a thousand time steps. The internal field V_{int} is included in the simulation. The doping density at the start of the simulation is set to 10^{18} cm^{-3}. The external potential at the interface $V_{ext}(L)$ produced by the split gates has the values 2.0 eV (solid lines), 1.0 eV (crosses), and 0.3 eV (boxes), respectively.

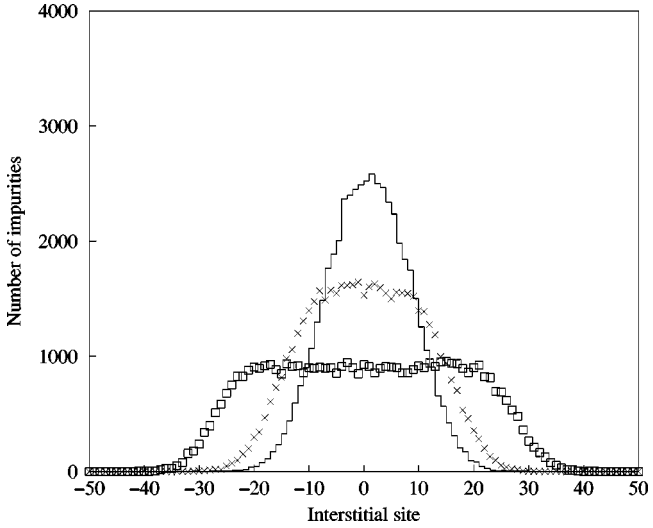

FIG. 5. The graph of the number of impurities at each interstitial site after a 50 (boxes), 100 (crosses), and 150 (solid line) time steps. The internal field V_{int} is not included in the simulation. The doping density at the start of the simulation is set to 10^{18} cm^{-3}. The external potential at the interface $V_{ext}(L)=2.0$ eV.

particles to flow out of the central region. The external potential dominates the total field after a certain distance from the center cause particle to flow into the central region. The flux into the central region reaches equilibrium with the flux out of the central region after several hundred time steps, thus no net flow of impurities occurs and the impurity density profile has stabilized. The width of the doped region is determined by the curvature of the parabola.

V. DISCUSSION

We have proposed an experiment to achieve controlled impurity diffusion using split gates. We believe that experi-

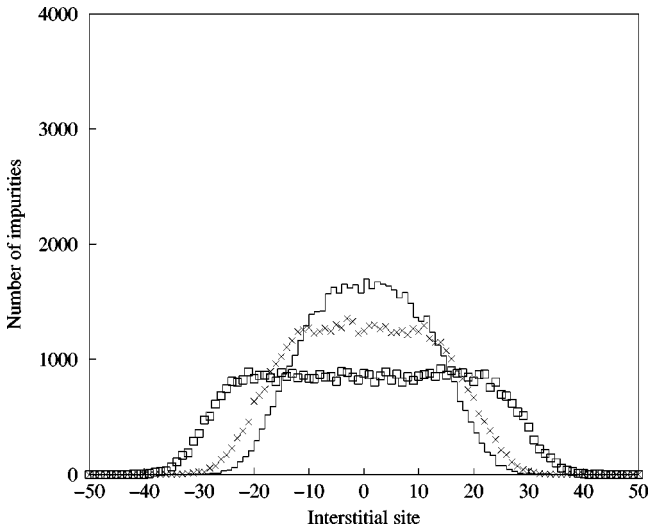

FIG. 6. The graph of the number of impurities at each interstitial site after a 50 (boxes), 100 (crosses), and 150 (solid line) time steps. The internal field V_{int} is included in the simulation. The doping density at the start of the simulation is set to the constant value of 10^{18} cm^{-3}. The external potential at the interface $V_{ext}(L)=2.0$ eV.

ments are best performed for ionized impurities that diffuse through the interstitial mechanism that has a much lower activation energy than other diffusion mechanisms. We have described a purely phenomenological model that could be verified by experiment. We calculated the internal field without taking into account the discrete nature of the charge distribution. We believe this model accurately describes long range impurity-impurity interactions. However, the true internal potential can contain large random potentials in the vicinity of a given impurity caused by short range impurity interactions. The random potentials have a greater chance of occurring with increasing doping density, which may cause broadening of δ-doped layers after a critical doping density.[21] The random potential we expect for our system will resist the build up of charge driven by the external potential, and will broaden the impurity profile. We believe however, the trends predicted in our model are correct, and the inclusion of the random potentials shall be a further refinement of the model. The random potentials shall only be important after a certain critical doping density, this doping level can only be accurately found by a numerical study.

The ideas described here can be used to facilitate the minaturisation of devices such as the NMOS and PMOS which are vital components of computer chips. A set of split gates strategically orientated, can be employed to restricted donor and acceptors in standard MOS devices, such that high fields could produce sharp doping profiles, allowing further device minaturisation. Furthermore, it could be advantageous to leave these split gates that are not necessary for device performance, so that device degradation (such as contamination of the oxide layer) could be reversed at a later date with a combination heat treatment and the field effect from the split gates.

ACKNOWLEDGMENTS

This work was funded by the TMR network (Contract No. ERB4061PL95) of the fifth framework program of the European Union. V Narayan would like to thank M. Yousif, I. Choquet, J. Vincent and P. Sundqvist for useful discussions.

[1] G. E. Murch and A. S. Nowick, *Diffusion in Crystalline Solids* (Academic Press, Orlando, Florida, 1984).
[2] J.A. Combs and C. Kunz, Phys. Rev. B **36**, 289 (1987).
[3] W.G. Kleppmann and R. Zeyher, Phys. Rev. B **22**, 6044 (1980).
[4] S. Fujii and Y. Uemura, Phys. Rev. B **40**, 1095 (1976).
[5] H.A. Kramers, Physica (Amsterdam) **7**, 284 (1940).
[6] S. Glasstone, K. J. Laidler, and H. Eyring, *The Theory of Rate Processes* (McGraw-Hill, New York, 1941).
[7] S. Chandrasekar, Rev. Mod. Phys. **15**, 1 (1943).
[8] G. Vineyard, J. Phys. Chem. Solids **3**, 121 (1957).
[9] W. Windl, M.M. Bunea, R. Stumpf, S.T. Dunham, and M.P. Masquelier, Phys. Rev. Lett. **83**, 4345 (1999).
[10] J. R. Manning, *Diffusion Kinetics for Atoms in Crystals* (Van Nostrand, London, 1968).
[11] M. Buttiker, E.P. Harris, and R. Landauer, Phys. Rev. B **28**, 1268 (1983).
[12] J.C. Severiens and C.S. Fuller, Phys. Rev. **92**, 1322 (1953).
[13] C.S. Fuller and J.C. Severiens, Phys. Rev. **96**, 21 (1954).
[14] E.M. Pell, J. Appl. Phys. **31**, 291 (1954).
[15] G. Popovici, T. Sung, S. Khasawinah, M.A. Prelas, and R.G. Wilson, J. Appl. Phys. **77**, 5625 (1995).
[16] T. Sung, G. Popovici, M.A. Prelas, R.G. Wilson, and S.K. Loyalka, J. Mater. Res. **12**, 1169 (1997).
[17] G. Popovici and M.A. Prelas, Diamond Relat. Mater. **4**, 1305 (1995).
[18] G. Popovici, T. Sung, and M.A. Prelas, J. Chem. Vap. Deposition **3**, 115 (1994).
[19] Y. Sun, G. Kirczenow, A.S. Sachrajda, and Y. Feng, J. Appl. Phys. **77**, 6361 (1995).
[20] A. Kumar, S.E. Laux, and F. Stern, Phys. Rev. B **42**, 5166 (1990).
[21] N.S. Averkiev, A.M. Monakhov, A. Shik, P.M. Koenraad, and J.H. Wolter, Phys. Rev. B **61**, 3033 (2000).
[22] H. Gould and J. Tobochnik, *An Introduction to Computer Simulation Methods* (Addison-Wesley, England, 1988), Pt. 2.
[23] A. B. Walker and K. O. Jensen (private communication).
[24] V. Narayan, BSc Dissertation, University of East Anglia, Norwich, England (1991).
[25] E. F. Schubert, *Doping in III–V Semiconductors* (Cambridge University Press, England, 1993).
[26] S. M. Sze, *VLSI Technology* (McGraw-Hill, London, 1988).
[27] V. Narayan and M. Willander (unpublished).
[28] A. Arnold, P. Markowich, and G. Toscani, Transp. Theory Stat. Phys. **29**, 571 (2000).
[29] A.A. Moya, A. Hayas, and J. Horno, Solid State Ionics **2**, 9 (2000),